Performance Studies of Heterogeneous Ion Exchange Membranes in the Removal of Bivalent Metal Ions in an Electrodialysis Stack

P. Ray

Reverse Osmosis Discipline, Central Salt and Marine Chemicals Research Institute (CSIR), Gijubhai Badheka Marg, Bhavnagar 364002, India

Received 18 July 2008; accepted 21 December 2008
DOI 10.1002/app.29983
Published online 2 April 2009 in Wiley InterScience (www.interscience.wiley.com).

ABSTRACT: Heterogeneous anion and cation exchange membranes have been prepared by solution casting technique with poly(vinyl chloride) as inert binder and anion/cation exchange resins (−300 + 400 mesh) in a blend ratio of 60 : 40. The membranes were characterized with respect to their physical, mechanical, and electrochemical behavior. Anion and cation exchange membranes (10 cell pairs) were packed in an electrodialysis stack in a parallel plus series flow pattern. Desalting experiments were carried out with four different salt solutions, such as calcium chloride, magnesium chloride, cupric chloride, and nickel chloride (varying in their total dissolved solid from 500 to 1000 ppm), at different applied potentials and flow rates. The resultant current, percentage reduction in total dissolved solid, current efficiency, and energy consumption were calculated. The maximum current density in the electrodialysis stack was observed for calcium chloride solution and at any applied potential and flow rate the percentage reduction in total dissolved solid for $Ca^{++} > Cu^{++} > Ni^{++} > Mg^{++}$. © 2009 Wiley Periodicals, Inc. J Appl Polym Sci 113: 1155–1164, 2009

Key words: membranes; ion exchangers; blends; poly (vinyl chloride); swelling

INTRODUCTION

Membrane processes are gaining lot of interest in the field of separation science and technology. Electrodialysis (ED)—one of the most important separation techniques, using ion exchange membranes—has versatile applications in food, chemicals, and drug industries.[1–5] At the same time, ED has been extensively applied for the desalination of brackish water and seawater.[6–11] It is particularly suited to applications that demand high product purity and at the same time plays a vital role in the field of industrial fluid treatment. The success of the ED process is highly dependent on the characteristics of the ion exchange membranes used in it.

Ion exchange membranes are electrolytic conductors due to the presence of ionic groups in them. Such membranes are classified into anion and cation exchange membranes, depending on the type of ionic groups attached to the membrane matrix. Cation exchange membranes contain negatively charged groups, such as $–SO_3^-$, COO^-, $–PO_3^{2-}$, PO_3H^-, $—C_6H_4O^-$, etc., fixed to the membrane backbone, and allow the passage of cations but reject anions. Anion exchange membranes contain positively charged groups, such as $–NH_3^+$, $–NHR_2^+$, $—NR_2H^+$, $–NR_3^+$, $–PR_3^+$, $–SR_2^+$, etc., fixed to the membrane backbone and they allow the passage of anions but reject cations.[12,13] According to the embedment of charged groups to the matrix or their chemical structure, ion exchange membranes can be further classified into homogeneous, in which the charged groups are chemically bonded to the membrane matrix, and heterogeneous, where the charged group bearing polymer is physically mixed with the binder matrix, respectively.

Both homogeneous and heterogeneous membranes compete with each other in different aspects. Homogeneous membranes possess excellent electrochemical properties but they lag in their mechanical strength, whereas heterogeneous membranes are excellent in their mechanical strength but comparatively poor in their electrochemical properties. Heterogeneous ion exchange membranes may be prepared by a combination of ion exchange resin particles with suitable binder either by calendaring or by dry molding of the resin and binder and by subsequently milling the mold stock or by solution-casting technique.[14,15]

The present work is aimed at the preparation of heterogeneous ion exchange membranes by solution casting technique and to study the relative transport

Correspondence to: P. Ray (paramita022002@yahoo.co.in).
Contract grant sponsor: The Ministry of Environment and Forests, India.

of different environment polluting bivalent metal ions through such membranes in an ED process. The transport of Ca^{++}, Mg^{++}, Cu^{++}, and Ni^{++} ions from their chloride salts have been studied under different experimental conditions and concentrations by varying the applied potential and flow rates. Water hardness, which is caused by the dissolved sulfates and chlorides of calcium and magnesium, is known as permanent hardness. Hard water is probably the most common water problem found not only at home but also in industry. In industry, hard water results in scaling in boilers, cooling towers, pipelines, and other industrial equipment. In the industrial setting, water hardness must be constantly monitored to avoid costly breakdowns. In the home environment, hard water causes many potentially costly problems. Copper has become a widespread pollutant due to its use as algaecide and fungicide in agriculture. Excessive intake of copper results in harmful diseases in both plants and animals. Both copper and nickel may be recovered from electroplating wastewater through ED using ion exchange membranes and the recovered metals may be reused in the plating bath, whereas the water may be recycled in the process.

MATERIALS AND METHODS

Materials

Poly(vinyl chloride) (PVC), 67 GEF092, *K* value 67, flexible lamination film grade, was supplied by IPCL (India).

Tetrahydrofuran, as solvent, with a refractive index of 1.407–1.409 and a density of 0.886–0.888 g/cm^3 at 25°C, anion exchange resin (Indion FFIP), a chloromethylated and aminated polystyrene (cross-linked with Divinyl benzene with 8% cross-link density) with an exchange capacity of 3.4 mequiv/g dry resin and cation exchange resin (Indion 225), a sulphonated polystyrene (cross-linked with divinyl benzene with 8% cross-link density) with an exchange capacity of 4.2 mequiv/g dry resin was supplied by Ion Exchange India, Ltd. (India).

Sodium chloride, anhydrous calcium chloride, magnesium chloride, $MgCl_2{\cdot}6H_2O$, cupric chloride, $CuCl_2$, all of purity $>$ 98% were acquired from E. Mark (Mumbai, India) and nickel chloride, $NiCl_2{\cdot}6H_2O$, with 97% purity was acquired from SD Fine Chemicals (India).

The reagents like silver nitrate and EDTA used for analysis were of analytical grade. Erichrome black T was used as an indicator.

Preparation of membranes

Both cation and anion exchange resin particles were dried in an oven at 60°C, for 24 h, and then ground to a very fine particle size (average particle size, 39 μm for anion exchange resin and 12 μm for cation exchange resin powder).[16,17] The powdered ion exchange resin was dispersed in solution of PVC in tetrahydrofuran (10% w/v) by retaining a resin : binder ratio of 60 : 40. Polyamide cloths with 37% open area and mesh opening of 130 μm was selected for the preparation of reinforced membrane. The membranes were prepared by dip-coating technique with the help of a membrane-casting machine. The membranes were dried at an ambient temperature (35°C) and the almost-dried membranes were immersed in water. The membranes were conditioned by equilibrating in 1*N* NaOH and subsequently in 1*N* HCl solutions.

Membrane characterization

Ion exchange capacity and moisture content

The cation and anion exchange membranes were regenerated by consecutive treatment with 1*N* NaOH and 1*N* HCl solutions (three times each) and washed thoroughly with deionized water to make them acid-free. The membranes in H^+ (cationic)/Cl^- (anionic) forms were mopped with blotting paper (to remove externally adhere moisture) and cut into two pieces. One piece was kept in a weighing bottle, which along with its lid was already weighed (W_1). The weighing bottle (with lid) and the piece of mopped membrane were again weighed (W_2) and kept in an electrical oven at 105°C for 3 h. The dried membrane in the bottle was then kept in desiccators for 30 min and weighed again (W_3). From the loss of weight, the percentage of moisture content of the membrane was calculated as follows:

$$\text{Moisture content} = \frac{W_2 - W_3}{W_2 - W_1} \times 100\%$$

Another piece of membrane was directly weighed (W_c) and equilibrated with 50 mL solution of 1*N* KCl (for cationic) and 1*N* KNO_3 (for anionic) in a stoppard glass bottle for 24 h. The amount of H^+ ion (for cationic) and Cl^- ion (for anionic) displaced was then determined analytically by titrating suitable aliquots from the equilibrium solution with standard 0.1*N* NaOH/$AgNO_3$ solution, respectively,

$$\text{Capacity} = \frac{V_1 S V_e}{W_c(100 - M)V} \times 100\,\text{meq/g dry membrane}$$

where V is the volume of aliquot taken for titration; V_1 and S are titer volume and strength of NaOH/$AgNO_3$, respectively, and V_e is the volume of 1*N* KNO_3 taken for equilibrium = 50 mL.

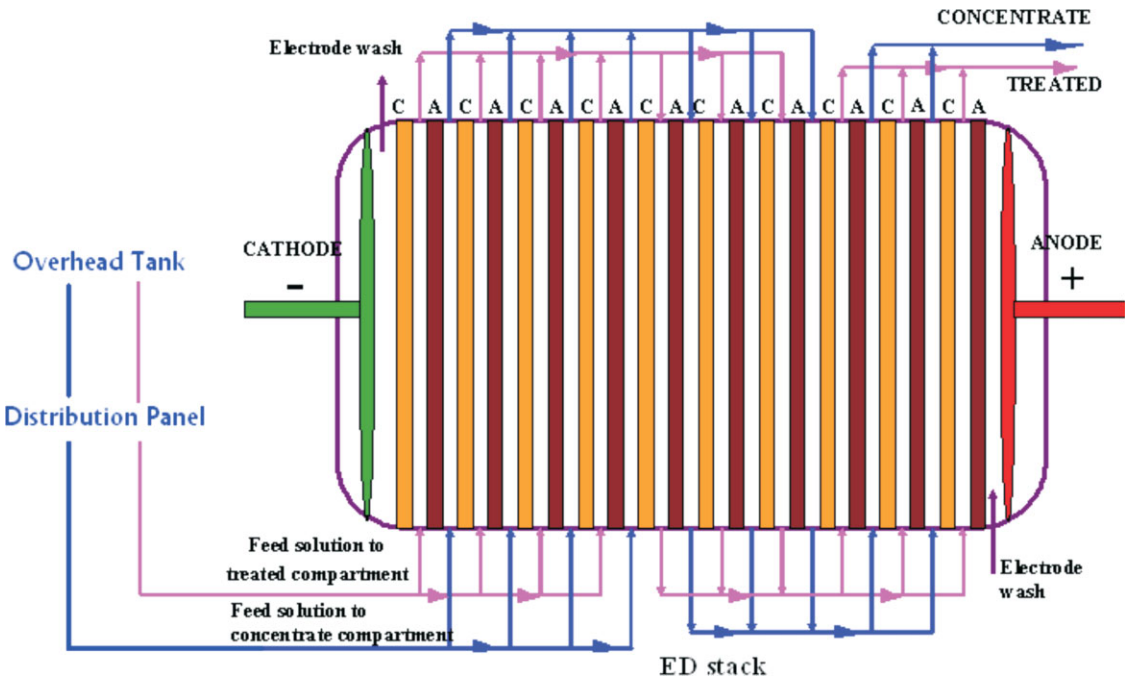

Scheme 1 Schematic layout of the ED process. [Color figure can be viewed in the online issue, which is available at www.interscience.wiley.com.]

Resistance

The ion exchange membranes were converted to suitable ionic form (H^+ for cationic and Cl^- for anionic) and washed with deionized water. The electrical resistance of the membranes in electrolyte solution containing the same counter-ion as in the membrane was then measured. Two half-cells of Perspex with a cross-sectional area of 1.228 cm^2 connected in series for solution flow were used with a resistance bridge to measure the areal resistance of the membrane samples in respective ionic form using the electrolyte solution under test. The electrical resistance of the solution in the cell with and without membranes was measured. The difference of the electrical resistance gave the membrane resistance. Membrane resistance multiplied by the cross-sectional area of the cell gave the areal resistance. The process was repeated until reproducible values within $\pm 0.1\ \Omega$ were obtained.

Transport number

Anion exchange membranes in Cl^- form were kept in 0.1*N* KCl solution for 2 h at 25°C. Membrane samples were then clamped between two Perspex half-cells fitted with calomel electrodes and stirring arrangements. The two halves of the cell were filled with 0.2*M* and 0.1*M* solution of KCl on either side of membrane. The potential developed due to the concentration difference was measured with a microvoltmeter. The transport number of membranes was calculated from the observed potential (V) and the theoretical concentration potential (V_0) as transport number $= (V + V_0)/2V_0$.[18]

Experimental setup

A schematic presentation of the experimental setup with 10 cell pairs of membranes is shown in Scheme 1. The salient features of the stack are given in Table I.

The ED stack was packed with 10 cell pairs of cation and anion exchange membranes. A parallel plus series flow in three stages was employed in the stack. The effective cross-sectional area of a single membrane was 81 cm^2. Salt solutions of different concentrations were taken to the overhead tank (Scheme 1). The solution was then passed through a distribution panel where it split into two different streams. One stream was fed to the treated compartments of ED stack, the outlet of which produced product water. The second stream was fed to the concentrate compartments, the outlet of which became concentrate. After the removal of air from the stack flow rate of treated and concentrate, streams were adjusted so that the flow rate of treated and concentrate remained 3 : 1. The electrical potential was applied to the ED stack through the rectifier and the resultant current was recorded for each salt solution. The experiments were carried out at different flow rates varying from 1 to 4.3 L/h at

TABLE I
Salient Features of the Electrodialysis Stack

1. No. of cell pairs	10
2. Membranes	Heterogeneous cation and anion exchange membranes
3. Size of membranes	15 cm × 10 cm
4. Effective cross-sectional area	81 cm^2
5. Cell thickness	0.2 cm
6. Gaskets	Built-in flow arrangement and spacers from HDPE
7. Electrodes	Cathode from SS sheet and anode from expanded titanium metal coated with precious metal oxide
8. Housing for electrodes	Rigid PVC with built-in flow distributor and outlets
9. Pressing assembly	Threading rods with nuts for leak proof assembly
10. Flow arrangement	Parallel plus series flow in three stages

three different applied potentials of 10, 15, and 20 V. After attaining a steady current for a particular flow rate, the product and concentrate water samples were analyzed. The calcium and magnesium ion content were estimated by EDTA titration by using Erichrome black T indicator and copper and nickel ion content were estimated by atomic absorption spectrophotometry method.

RESULTS AND DISCUSSION

Evaluation of membrane properties

The heterogeneous membranes prepared for the present experiments contain ion exchange resin particles distributed in the PVC matrix. The average properties of these membranes are presented in Table II. As it has been revealed from our previous experiments[16,17] that a blend composition of 60 : 40 resin : binder results in an optimum balance of mechanical, electrochemical, and morphological properties, hence, for the present experiment, this particular blend ratio has been selected.

Table II reveals that the membranes possess good electrochemical properties, which are highly suitable for desalination application.

Desalting application

The desalting performance of the ED stack was initially studied with sodium chloride solution (750 ppm) at different applied potentials (10–20 V) and flow rates (1.2–4.2 L/h). The flow rate ratio of treated and concentrate was maintained to have 75% water recovery. The results are presented in Table III.

The data showed that at any applied potential the current increases and percentage reduction in total dissolved solid decreases with an increase in flow rate. Similarly, at any particular flow rate enhancement in applied potential increases the desalting efficiency of the stack. It is seen from the table that product water of desired total dissolved solid (TDS) may be achieved with reasonable current efficiency and energy consumption by optimum balance of the operating parameters (i.e., applied potential and flow rate). More than 85% reduction in NaCl concentration could be achieved with this ED stack under set experimental conditions. These primary performance evaluation data helped us to select the stack for the removal of bivalent metal ions, which is discussed in the succeeding sections.

Removal of Ca^{++} (calcium chloride)

Calcium chloride solutions of three different concentrations (500, 750, 1000 ppm) have been selected for the present study. The desalination experiments have been carried out at three different applied potentials of 10, 15, and 20 V by varying the flow rate from 1.2 to 4.2 L/h. The results of the experiments have been presented graphically in Figures 1–4. It is observed from Figure 1 that at any fixed potential the current in the system increases with an increase in the flow rate. This is because an increase in the flow rate enhances the linear velocity, which reduces the probability of formation electrolyte deficient layers on the diluate side of membrane surface

TABLE II
Properties of Membranes PVC : Resin 60 : 40 (w/w)

Properties	Cation Exchange Membrane	Anion Exchange Membrane
Areal resistance (Ω cm^2)	10–12	15–16
Moisture content (%)	22.05	23.12
Capacity (mequiv/g)	1.182	1.127
Transport number	0.975	0.965

The average particle size of cation exchange (sulfonated polystyrene) and anion exchange resin (chloromethylated and aminated polystyrene) powders are 12 and 39μm, respectively.

TABLE III
Desalting Performance with Sodium Chloride Solution Feed Water NaCl Content 750 ppm, Flow Rate Ratio Treated : Concentrate 3 : 1

Exp. no.	Applied potential (V)	Flow rate of treated solution (L/h)	Current (mA)	Product water Cl^- as NaCl (ppm)	(%R)	CE (%)	energy (kWh/m^3)
1	10	1.2	60	175	76.7	51.77	0.50
		1.8	72	227	69.7	58.8	0.40
		3.1	89	292	61.1	71.8	0.29
		4.2	105	310	58.7	79.24	0.25
2	15	1.2	66	142	81.1	49.76	0.825
		1.8	78	191	74.5	58.10	0.65
		3.1	97	256	65.9	71.08	0.47
		4.2	115	290	61.3	75.56	0.41
3	20	1.2	70	108	85.6	49.52	1.16
		1.8	85	143	80.9	57.82	0.94
		3.1	110	208	72.3	68.76	0.71
		4.2	130	260	65.3	71.23	0.62

and hence the overall stack resistance decreases. As a result, at any particular potential, the current increases ($V = IR$) with an increase in flow rate (Fig. 1).

An ED stack resistance comprises different components (i.e., the cationic and anionic membrane resistance): the resistance of the liquids in concentrates and treated chambers, and extra resistance contributed by the spacer materials employed. The membrane and the spacer resistances are the inherent characteristics; hence, it remains almost unaffected with the progress of desalination. The resistance of the concentrate compartments is generally ignored as ED starts with a reasonably high concentration of solution in the concentrate compartments. It is the concentration of the treated chambers that plays a dominant role in controlling the resultant current in the system as this resistance gradually increases with desalination. The current taken in all the experiments is steady current.

Figure 2 depicts the variation of percentage reduction in salt content with flow rate. At any applied potential, the reduction in salt content decreases with an increase in flow rate as the enhancement in

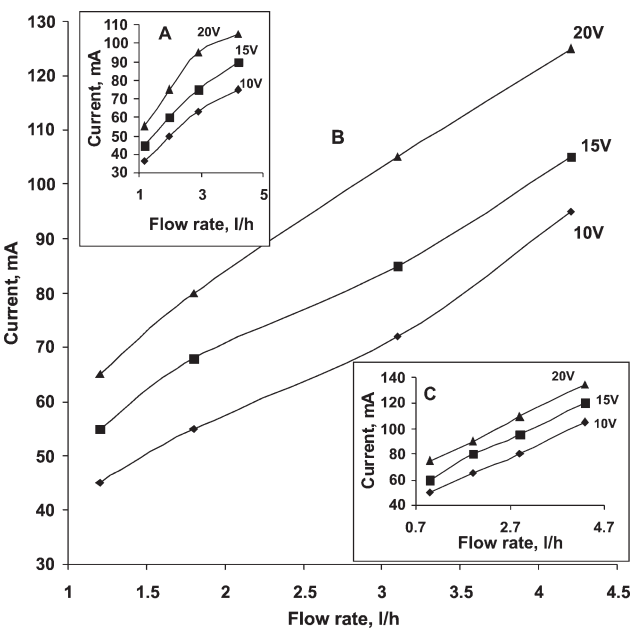

Figure 1 Current vs. flow rate for $CaCl_2$ solutions at different applied potentials. Area of each membrane, 81 cm^2; $CaCl_2$ concentration: A: 500 ppm; B: 750 ppm; C: 1000 ppm.

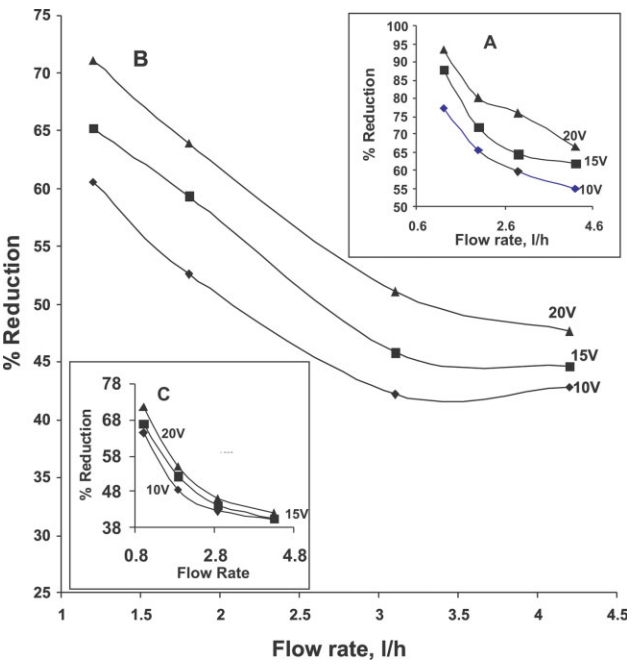

Figure 2 % Reduction vs. flow rate for $CaCl_2$ solutions at different applied potentials. $CaCl_2$ concentration: A: 500 ppm; B: 750 ppm; C: 1000 ppm.

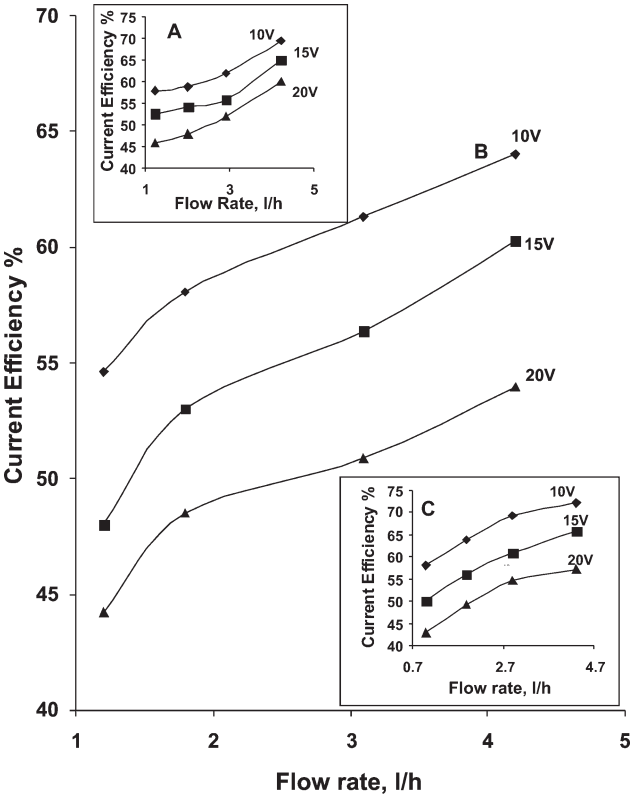

Figure 3 Current efficiency (%) vs. flow rate for $CaCl_2$ solutions at different applied potentials, $CaCl_2$ concentration: A: 500 ppm; B: 750 ppm; C: 1000 ppm.

the flow rate decreases the residence time of the solution in the stack. Hence, at a higher flow rate, the outlet concentration of the treated stream will be more than that of the treated stream at lower flow rate. A thorough observation (Fig. 2) reveals that the percentage reduction in TDS decreases by 20% (on an average) with an enhancement of treated flow rate from 1 to 4 L/h and it does not vary much with the change in applied potential and starting TDS. This indicates that the residence time is one of the prime parameters in the desalting performance of an ED stack.

The current efficiency (η) of an ED unit can be calculated as $\eta = 26.8(C_1 - C_2)Q/ni$, where i is the current density (I/A), n is the number of cell pairs, Q is the flow rate, C_1, C_2 are feed and product concentrations.[18]

The current efficiency is dependent on the properties (selectivity) of the membrane, the water transport through the membrane by osmosis and electro-osmosis, and leakage current. The selectivity is having a positive effect, whereas the electro-osmosis and leakage current negatively affect the current efficiency.[19] Current efficiency is a combined factor of percentage reduction in TDS, flow rate, and the resultant current in the system. It is seen from Figure 3 that at any applied potential current efficiency increases with an increase in flow rate and at any fixed flow rate current efficiency decreases with an increase in applied potential. Electric transference in the absence of diffusion is proportional to the current density and it is noted that the enhancement of flow rate results in higher current density. Hence, the current efficiency increases with flow rate. Enhancement of the applied potential by keeping the other parameters constant may enhance the water transport through membranes by electro-osmosis, which results in co-ion transport and, as a result, current efficiency decreases.

The energy required for the removal of a given amount of electrolyte depends not only on the current efficiency but also on the operating voltage. If the applied voltage is higher than the sum of the membrane potentials, then only a resultant current may cause further depletion in salt concentration in a dilute solution. This excess voltage required to attain the desired current density depends on the ohmic resistance of the cell. Energy is calculated as E (kWh/m^3) $= VI/L$, where V is the voltage (Volt), I is the current at steady state (Amp), and L is the volumetric flow rate (L/h) of the product stream. It is observed from Figure 4 that an enhancement of the applied potential results in higher energy consumption irrespective of the flow rate and starting TDS. However, at any starting TDS, higher flow rate results in a lower energy consumption because higher flow rate helps to remove the electrolyte deficient stagnant layer on the membrane surface formed during the course of ED, which in turn decreases the cell resistance.

REMOVAL OF Mg^{++}

Desalination of magnesium chloride solution of three different concentrations of 500, 750, and 1000 ppm has been carried out with the same ED stack used

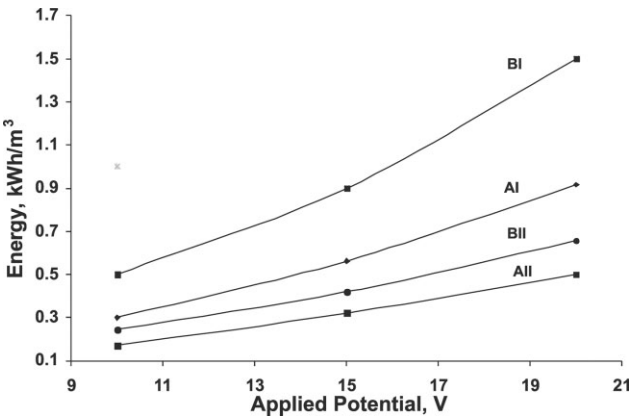

Figure 4 Energy consumption vs. applied potential for $CaCl_2$ solutions $CaCl_2$ concentration: A: 500 ppm; flow rate: I, 1.2 L/h; II, 4.2 L/h; B: 1000 ppm; Flow rate: I, 1.0 L/h; II, 4.3 L/h.

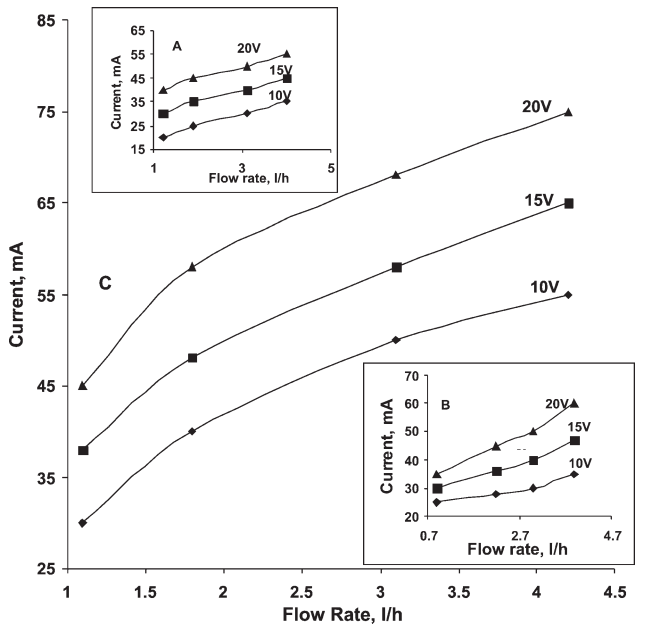

Figure 5 Current vs. flow rate for $MgCl_2$ solutions at different applied potentials. Area of each membrane, 81 cm^2; $MgCl_2$ concentration: A: 500 ppm; B: 750 ppm; C: 1000 ppm.

for calcium chloride solution. The results are presented in Figures 5–8. The trend of variation of different parameters like current (Fig. 5), percentage reduction in TDS (Fig. 6), and current efficiency (Fig. 7) is the same as in the case of calcium chloride solution. Enhancement of applied potential as well as flow rate results in the enhancement of current density. However, one of the salient observations is that, at any applied potential and flow rate, the resultant current in the system is always lower than that of calcium chloride solution at any particular TDS of the feed solution. This may be due to the fact that the equivalent conductance of Ca^{++} (59.5 mho cm^2/equivalent) is higher than that of Mg^{++} (53.06 mho cm^2/equivalent),[20] which results in a higher current density in the case of calcium chloride solution.

Because of the comparatively lesser current density, the achievable percentage reduction in TDS is lesser for the $MgCl_2$ solution than for the $CaCl_2$ solution. It is observed that for 500 ppm $MgCl_2$ solution the reduction in TDS is decreased by 24% with an enhancement of treated flow rate from 1.2 to 4 L/h at an applied potential of 1 V/cell pair, whereas the percentage reduction is decreased by 45% for the same change of flow rate at an applied potential of 2 V/cell pair. This indicates that, unlike $CaCl_2$ solutions, the applied potential plays a major role in addition to the residence time for $MgCl_2$ solutions at a low solute concentration. However, with the enhancement of solution concentration, the effect of potential gradually decreases.

For the $MgCl_2$ solution, even at a low current density, a reasonable percentage reduction could be

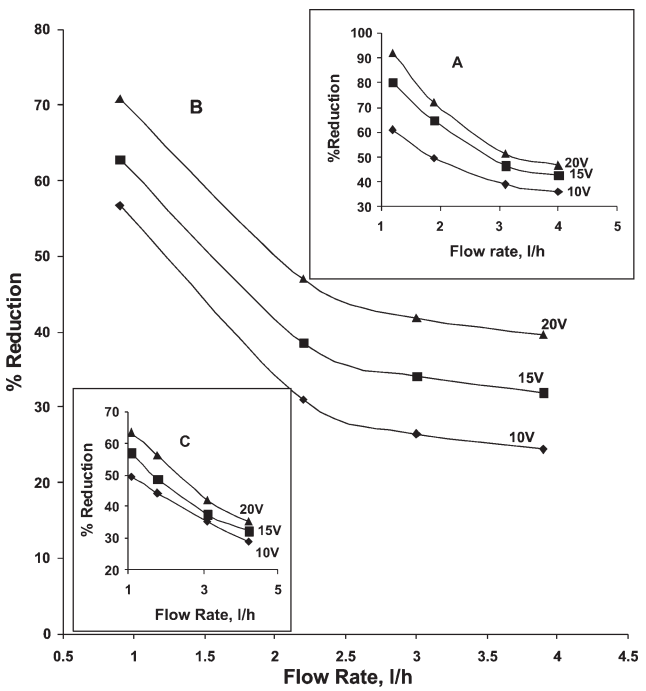

Figure 6 Percentage reduction vs. flow rate for $MgCl_2$ solutions at different applied potentials. $MgCl_2$ concentration: A: 500 ppm; B: 750 ppm; C: 1000 ppm.

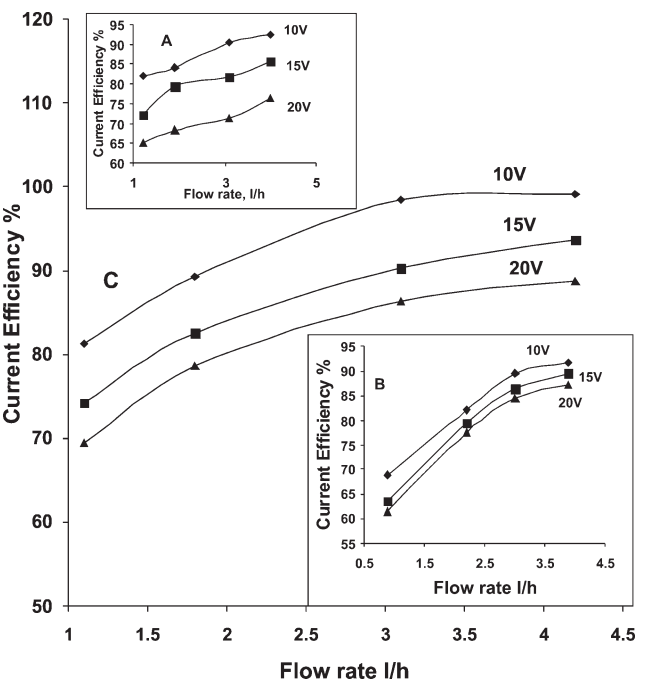

Figure 7 Current efficiency (%) vs. flow rate for $MgCl_2$ at different applied potentials. $MgCl_2$ concentration: A: 500 ppm; B: 750 ppm; C: 1000 ppm.

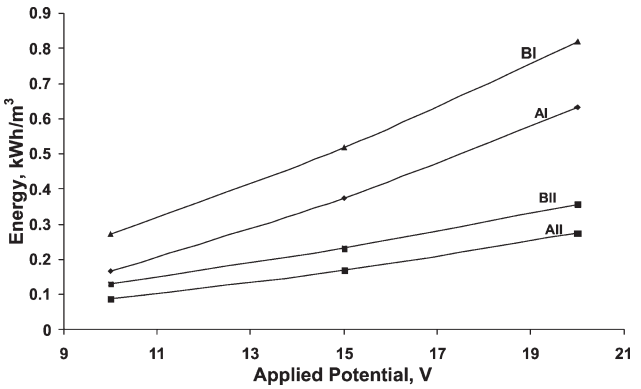

Figure 8 Energy consumption vs. applied potential for $MgCl_2$ solutions $MgCl_2$ concentration: A: 500 ppm; flow rate: I, 1.2 L/h; II, 4.0 L/h; B: 1000 ppm; flow rate: I, 1.1 L/h; II, 4.2 L/h.

achieved, which is reflected at a comparatively higher current efficiency for such solutions in comparison with $CaCl_2$ solution with the same initial TDS values. Enhancement of flow rate increases the current efficiency and at any particular flow rate an increase in potential decreases the current efficiency (Fig. 7). Similar to $CaCl_2$, here also the energy consumption decreases with an increase in flow rate (Fig. 8).

Removal of Cu^{++} and Ni^{++}

ED experiments have been carried out with $CuCl_2$ and $NiCl_2$ solutions of three different TDS, namely 1000, 750, and 500 ppm. As the trend of variation of different parameters like current, percentage reduction in TDS, current efficiency, and energy consumption remains almost the same for all the three TDS, hence the results of the starting TDS of 500 ppm for both the salts are presented here.

For the ED experiments of cupric chloride solutions, the general observations are quite conversant with those of Mg^{++} and Ca^{++}. At any particular flow rate, the enhancement of applied potential results in more current density in the stack, which in turn enhances the percentage reduction in TDS (Figs. 9 and 10). Similarly, the desalting efficiency of the stack decreases with the enhancement of flow rate at any fixed potential because of the decrease in residence time in the ED stack. It is known that the hydrated radius of Cu^{++} (6 Å) is the same as that of Ca^{++} (6 Å) but the limiting equivalent ionic conductance of Cu^{++} (55.0 mho cm^2/equivalent) is lesser than that of Ca^{++} (59.5 mho cm^2/equivalent).[20] Because of this, at any fixed potential and starting TDS the achievable current density for $CaCl_2$ solution is comparatively higher than that with $CuCl_2$ solution [Figs. 1(A) and 9]. Current in the ED stack is one of the most important factors for desalting and is reflected in the percentage reduction in TDS for these two salt solutions. If we compare the experimental results of $CaCl_2$ and $CuCl_2$ solutions with starting TDS of 500 ppm, it is observed that for all the different applied potentials and flow rates the percentage reduction of TDS is always higher for $CaCl_2$ solutions in comparison with $CuCl_2$ solutions [Fig. 2(A) and 10].

The variation of current efficiency with flow rate is shown in Figure 11. The trend is the same as observed in the case of the previous two salt solutions. At any applied potential and starting solution TDS, the energy consumption is directly proportional to the resultant current in the system and inversely proportional to the flow rate. The energy consumption for desalting of $CuCl_2$ solution is

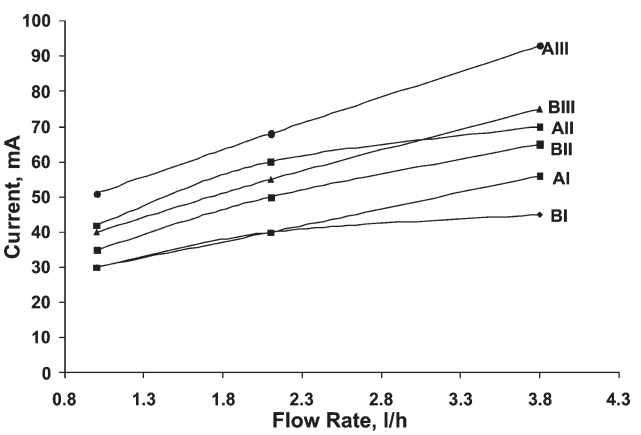

Figure 9 Variation of current with flow rate at different applied potential. Area of each membrane, 81 cm^2. A: $CuCl_2$ and B: $NiCl_2$ solutions each of 500 ppm TDS. Applied potential, I, 10 V; II, 15 V; III, 20 V.

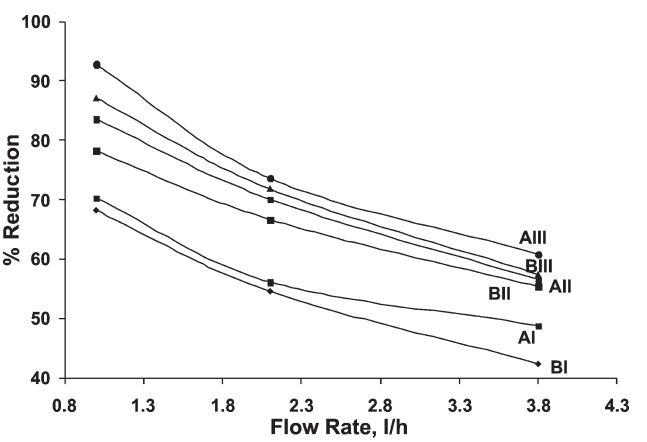

Figure 10 Variation of percentage reduction with flow rate at different applied potentials. A: $CuCl_2$ and B: $NiCl_2$ solutions each of 500 ppm TDS. Applied potential, I, 10 V; II, 15 V; III, 20 V.

comparable and in most of the cases lesser than that of $CaCl_2$ solutions because of the lesser resultant current at any fixed flow rate and applied potential [Figs. 4(A) and 12].

Experimental results for the desalting of $NiCl_2$ solution by ED are also presented in Figures 9–12. The basic trends for the variation of different parameters like current (Fig. 9), percentage reduction (Fig. 10), CE% (Fig. 11), and energy consumed in the process (Fig. 12) are the same as observed for the other three salts. The limiting equivalent ionic conductivity (50.0 mho cm^2/equivalent) of Ni^{++} is least among the four selected ions[20]; hence, the percentage reduction, resultant current, and energy consumption for such system are lesser than that of Ca^{++} and Cu^{++} ions but observed to be more than Mg^{++}. Current efficiency increases with flow rate at any applied potential.

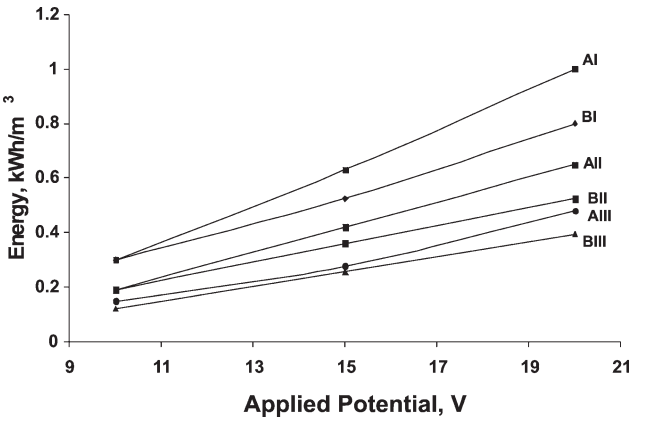

Figure 12 Variation of energy with flow rate at different applied potentials. A: $CuCl_2$ and B: $NiCl_2$ each of 500 ppm TDS. Flow rate: I, 1.0 L/h; II, 2.1 L/h; and III, 3.8 L/h.

Comparative evaluation of ED process in the removal of four different ions

We may have a comparative discussion on desalting of four different salt solutions by ED. At any specific concentration of the salt solution and applied potentials, the maximum current density could be achieved for $CaCl_2$ solutions, which may be attributed to the highest limiting equivalent ionic conductivity of Ca^{++} ion among the four. At the same time the maximum reduction in salt concentration also could be achieved for $CaCl_2$ solution. Desalting by ED depends not only on the ionic mobility but also the selectivity coefficients play a major role in the process. At equilibrium, the concentration of ions in solution and in the ion exchange resin particle is related through the selectivity coefficient, which may be defined as $S = [M^{n+}]_r[H^+]/[M^{n+}][H^+]_r$, where the subscript r refers to the resin phase. For a cation exchanger (made of polystyrene and divinyl benzene with 8% crosslink density) in the H form, the selectivity coefficient for Ca^{++} (1.8) is highest among the four selected ions. The respective values for Mg^{++}, Cu^{++}, and Ni^{++} are 1.15, 1.35, and 1.37, respectively.[20] Hence, both the ionic mobility and the selectivity favor the maximum desalting in case of calcium salts. Cu^{++} follows the limiting equivalent ionic conductivity of Ca^{++}, which possesses the same hydrated ionic radius as Ca^{++} (i.e., of 6 Å). Hence, the percentage reduction and resultant current for $CuCl_2$ solutions is just below the calcium salt solutions. Mg^{++} possesses the highest hydrated ionic radii among the four (8 Å) and its limiting equivalent conductivity is lesser than that of Ca^{++} and Cu^{++} ions (53.06 mho cm^2/equivalent). Moreover, the selectivity coefficient for Mg^{++} is the least in the four. Hence the percentage reduction in TDS for $MgCl_2$ salt is the lowest. Although the limiting equivalent conductivity of Ni^{++} is the lowest among the four, a comparatively lesser hydrated ionic radii (6 Å) and better selectivity coefficient of Ni^{++} compared to Mg^{++} favors its permeation through the membrane and as a result the percentage reduction in Ni^{++} ion concentration is better than that of Mg^{++}.

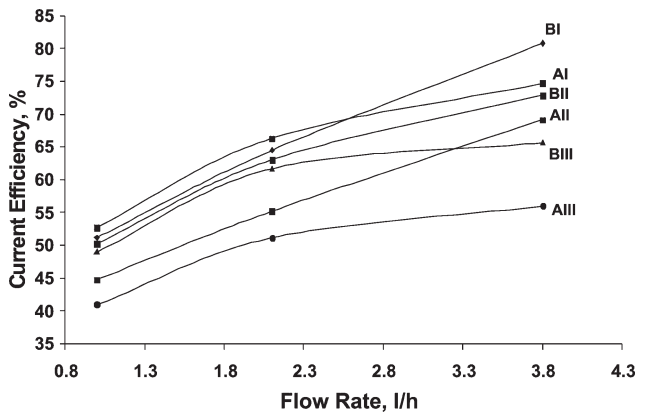

Figure 11 Variation of CE % with flow rate at different applied potentials. A: $CuCl_2$ and B: $NiCl_2$ solutions each of 500 ppm TDS. Applied potential, I, 10 V; II, 15 V; III, 20 V.

CONCLUSIONS

The ED process has been applied for the removal of four different bivalent metal ions (Ca^{++}, Cu^{++}, Ni^{++}, and Mg^{++}) from their solutions. It is observed that at any fixed flow rate enhancement in applied potential results in more reduction of salt. Current efficiency increases with an increase in flow rate at any applied potential and at any fixed flow rate current efficiency decreases with an increase in applied potential. Energy consumption increases with an

increase in percentage reduction at any fixed flow rate. At any applied potential and flow rate, the resultant current and the percentage reduction for $Ca^{++} > Cu^{++} > Ni^{++} > Mg^{++}$ and their output rate decreases following the same trend at any applied potential to achieve the same percentage reduction. The maximum current density and reduction in salt concentration for $CaCl_2$ solution is due to the highest limiting equivalent ionic conductivity and selectivity coefficient of Ca^{++} ion among the four. Highest hydrated ionic radii and least selectivity coefficient of Mg^{++} ion among the four are responsible for the lowest reduction in salt concentration for $MgCl_2$ solution.

References

1. Shah, B. G.; Trivedi, G. S.; Ray, P.; Adhikary, S. K. Sep Sci Technol 1999, 34, 3243.
2. Vyas, P. V.; Shah, B. G.; Trivedi, G. S.; Gaur, P. M.; Ray, P.; Adhikary, S. K. Desalination 2001, 140, 47.
3. Lee, E. G.; Moon, S. H.; Chang, Y. K.; Yoo, I. K.; Chang, H. N. J Membr Sci 1998, 145, 53.
4. Grib, H.; Belhocine, D.; Lounici, H.; Pauss, A.; Mameri, N. J Appl Electrochem 2000, 30, 259.
5. Elisseeva, T. V.; Shaposhnik, V. A.; luschik, I. G. Desalination 2002, 149, 405.
6. Harkare, W. P.; Adhikary, S. K.; Narayanan, P. K.; Bhayani, V. B.; Dave, N. J.; Govindan, K. P. Desalination 1982, 42, 97.
7. Mahabala, R. A.; Adhikary, S. K.; Narayanan, P. K.; Harkare, W. P.; Gomkale, S. D.; Govindan, K. P. Desalination 1987, 67, 59.
8. Adhikary, S. K.; Tipnis, U. K.; Harkare, W. P.; Govindan, K. P. Desalination 1989, 71, 301.
9. Adhikary, S. K.; Narayanan, P. K.; Thampy, S. K.; Dave, N. J.; Chauhan, D. K.; Indusekhar, V. K. Desalination 1991, 84, 189.
10. Song, S.; Pei, Q. C. Desalination 1983, 46, 191.
11. Thampy, S. K.; Narayanan, P. K.; Harkare, W. P.; Govindan, K. P. Desalination 1988, 69, 261.
12. Hideo, K.; Tsuzura, K.; Shimizu, H. In Ion Exchangers; Dorfner, K., Ed.; Walter de Gruyter: Berlin, 1991, 596.
13. Strathmann, H. In Membrane Separation Technology-Principles and Applications; Nobe, R. D., Stern, S. A., Eds.; Elsevier Science B.V.: Amsterdam, 1995; pp 214–278.
14. Winston, W. S. H.; Sarkar, K. K. Membrane Handbook; Van Nostrand Reinhold: New York, 1992.
15. Nagarale, R. K.; Shahi, V. K.; Rangarajan, R. J Membr Sci 2005, 248, 37.
16. Vyas, P. V.; Shah, B. G.; Trivedi, G. S.; Ray, P.; Adhikary, S. K.; Rangarajan, R. J Membr Sci 2001, 187, 39.
17. Vyas, P. V.; Shah, B. G.; Trivedi, G. S.; Ray, P.; Adhikary, S. K.; Rangarajan, R. React Functional Polym 2000, 44, 101.
18. Belfort, G. Synthetic Membrane Processes: Fundamentals and Water Applications; Academic Press: London, 1984.
19. Wilson, J. R. Demineriliazion by Electrodialysis; Butterworths Science Publication: London, 1960.
20. Dean, J. A., Ed. Lange's Handbook of Chemistry; McGraw-Hill: Singapore, 1987.